GEOPHYSICAL RESEARCH LETTERS, VOL. 17, NO. 1, PAGES 61-64, JANUARY 1990

WAVE-INDUCED BURST PRECIPITATION EVENTS DETECTED WITH A DIGITAL IONOSONDE

M. J. Jarvis and A. J. Smith

British Antarctic Survey, Natural Environment Research Council

F. T. Berkey

Center for Atmospheric and Space Sciences, Utah State University

D. L. Carpenter

STAR Laboratory, Stanford University

Abstract. Initial results are presented from two methods whereby burst precipitation events in the lower ionosphere, almost certainly induced by VLF wave-particle interactions in the magnetosphere, have been detected using a ground-based digital ionosonde. In the first method, HF echoes are received above the critical frequency of the surrounding plasma; particle energies and the location and extent of the plasma enhancement may be deduced. In the second method, a rapid decrease in the phase of ionospheric echoes is observed due to refractive index changes along the echo path; particle energies, the duration of the precipitation event and the precipitation energy flux can be estimated.

Introduction

An important class of magnetospheric wave-particle interactions is believed to involve the cyclotron resonance mechanism. Cyclotron resonance occurs when the Doppler-shifted frequency of a VLF wave, in the reference frame of the counterstreaming electrons, equals the electron gyrofrequency [see e.g. Helliwell, 1969]. As a result, the pitch angle of a resonant electron is modified, either up or down, depending on the initial conditions of the interaction. If the pitch angle of an electron falls within the loss cone, then there is a very high probability that it will be precipitated into the ionosphere by collisional processes. This electron precipitation has been observed both *in situ* and remotely in the past using a number of techniques.

Rycroft [1973] first reported an *in situ* measurement aboard a sounding rocket at an altitude of 100 km at an L-value of ≈3.3. During this event, both >45 keV and 110 keV electron detector channels recorded an enhanced electron intensity event ≈20 times greater than the background level. The event lasted ≈6 s during which time two-, four-, six-, and eight-hop whistlers were recorded on the ground. Voss et al. [1984] reported on several similar events recorded *in situ* by a satellite at L≈2.3, establishing a one-to-one correlation between a series of strong electron bursts and one-hop whistler traces recorded concurrently on the ground.

Remote detection has been achieved by Rosenberg et al. [1971], using X-ray detectors aboard a balloon, by Helliwell and Mende [1980], using ground-based photometers at L≈4 and via the Trimpi effect, whereby short-lived localised ionisation enhancements in the *D*-region cause amplitude and phase perturbations in radio transmissions with propagation paths passing within the vicinity of the enhancement [e.g. Carpenter et al., 1984]. Inan et al. [1985] attributed these perturbations to a reduction of 0.1-1 km in the effective reflection height of ground-launched VLF waves (nominally ≈85 km) and estimate particles fluxes of 10^{-3} to 10^{-2} ergs cm^{-2} s^{-1}. Carpenter and LaBelle [1982], by comparison of Trimpi events on different propagation paths, have estimated that individual ionospheric perturbations from such events extend ≈100 km in the East-West direction.

The data presented herein were recorded at Halley (76°S, 27°W) (method 1) and Siple Station (76°S, 84°W) (method 2), Antarctica; both stations have similar L values (≈4.2). The digital ionosondes employed are NOAA HF radars [Grubb, 1979]. These have the advantage over conventional ionosondes of providing not only the time-of-flight and amplitude of each echo return, but other echo parameters including wave polarisation sense, 'skymap' echo location and effective line-of-sight Doppler velocity [e.g. Jarvis and Dudeney, 1986]. The instrument operates in both swept-frequency ionogram and fixed-frequency kinesonde modes. In the latter, several frequencies are repeated continuously on a cyclic basis to produce concurrent time series of transmitted pulses on several frequencies. It is data from these kinesonde soundings which are used in this paper.

Paper number 89GL03594.
0094-8276/90/89GL-03594$03.00

Method 1: Direct Echo Reflection From Ionisation Enhancements

The kinesonde frequencies are arranged so that at least one of them (f_n) is just above the critical frequency of the *E*-region. Thus, under steady background conditions, no echoes are returned at that frequency. A short-lived electron density enhancement will, if it is advantageously positioned and oriented, reflect the HF waves transmitted by the ionosonde to produce a burst of echo returns on frequency f_n.

For the example shown here, recorded at Halley on 23 June 1982 at ≈2020 UT, the critical frequency of the *E*-region for extraordinary mode echoes was just below 2.6 MHz (estimate by interpolating between digital ionograms is 2.595 ±0.01 MHz). One kinesonde frequency, f_n, was set to 2.602 MHz and was sampled at intervals of 0.48 s with a total duration of 240 s.

Figure 1 shows the range, deduced from echo time-of-flight, of the only ionosonde echoes (all extraordinary mode) received from below 200 km on 2.602 MHz during one complete sounding. Note that timing synchronization between experimental data sets at Halley

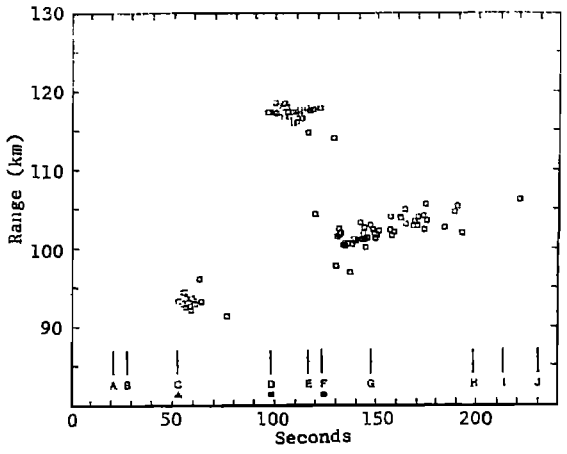

Fig. 1. A virtual range-time plot for a kinesonde sounding recorded at Halley, Antarctica on 23 June 1982. The times which correspond to whistlers observed during this 240 second interval have been identified on the time axis. The sounding started at 2017:47 UT and the data shown here were obtained on 2.6 MHz.

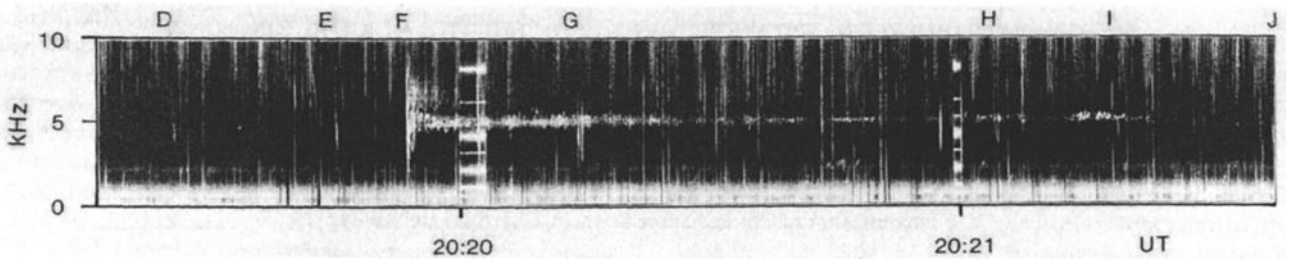

Fig. 2. The Halley VLF spectrogram for the interval 2019:30-2021:30 UT on 23 June 1982, identifying the whistler emissions (D,F) associated with HF echoes.

is of the order of one second. The VLF spectrogram, Figure 2, for part of the same period is typical of the type of VLF activity prevalent at around this time. Individual whistlers are marked with the same lettering as used in Figure 1. Whistlers A, B and C (not shown in Figure 2) were almost identical in nature to D. A very strong whistler (labelled F) with triggered emissions at around 5 kHz can be seen just before 2020 UT. Also apparent are a number of weaker whistlers (D,E,G,H,I and J) although I and J are so weak as to be almost indiscernible. There are three distinct bursts of echoes on the ionosonde, each with a significantly different range; the commencement of these bursts coincides with the reception of whistlers C, D and F. The burst of echoes associated with whistler F is longest lived and approximately coincides in length with the duration of the triggered emissions associated with that whistler. Thus there is strong evidence that the bursts of ionisation enhancement are directly associated with whistlers C, D and F. There is no indication of any ionospheric echoes associated with the other whistlers. Closer inspection of the whistler spectrograms reveals no significant difference between those whistlers which have apparently produced evidence of precipitation on the ionosonde and those which have not. Possible explanations are that not all the whistlers are occurring at the same longitude, that the level of precipitation is dependent upon rapidly changing wave-particle interaction parameters, or that the physical shape of the enhancement may not always allow specular reflection of transmitted signals back to the ionosonde. In order to be detected in this example, the enhancement has to lead to an increase in plasma frequency from <1.874 MHz to 1.882 MHz, equivalent to an electron density increase of $>360\times10^6$ m^{-3} (from $<43.02\times10^9$ m^{-3} to 43.38×10^9 m^{-3}). This requires a flux at least an order of magnitude greater than that required to produce the increase of 37×10^6 m^{-3} given by Inan et al. [1985] for a Trimpi event. An alternative is that irregularities in electron density distribution of a turbulent or quasi-stratified nature, induced by the precipitation, might be responsible for the reflections [Belrose, 1970], in which case the flux cannot be directly determined.

The separation in range of each distinct echo burst (Figure 1) is mainly due to each occurring at a different geographical position. Figure 3 shows the 'skymap' locations of the echoes; each of the echo bursts has been plotted with a different symbol (that marked against the causative whistler time on Figure 1). The mean altitudes of each echo burst, calculated assuming straight line propagation, are ≈86, ≈85 and ≈92 km respectively for whistlers C, D and F. Taking these heights to be the altitude of maximum ionisation rate of the precipitated electrons, then they indicate initial electron energies of ≈70, ≈80 and ≈40 keV respectively [Banks et al., 1974].

During the interval 2000 to 2045 UT on 23 June 1982, many bursts of ionisation enhancement were observed on the ionosonde. The level of VLF activity was so high, however, that for much of the time it was impossible to link a particular ionisation enhancement positively with any one whistler or emission. There were, however, eight occasions when a lull in VLF activity around the time of the burst enable reliable causal identification.

The three events in Figure 3 were typical of all eight in that the echoes from each burst covered an area between 30 and 100 km across. Patches of pulsating aurora having dimensions of ≈75 by 250 km (elongated in the east-west direction) were associated with VLF chorus emissions at L≈4.4 by Tsuruda et al. [1981]. Some care has to be taken in interpreting the area covered by each echo burst on the 'skymap' plot (e.g. Figure 3) in terms of the actual size of the electron enhancement. The apparent size will depend upon

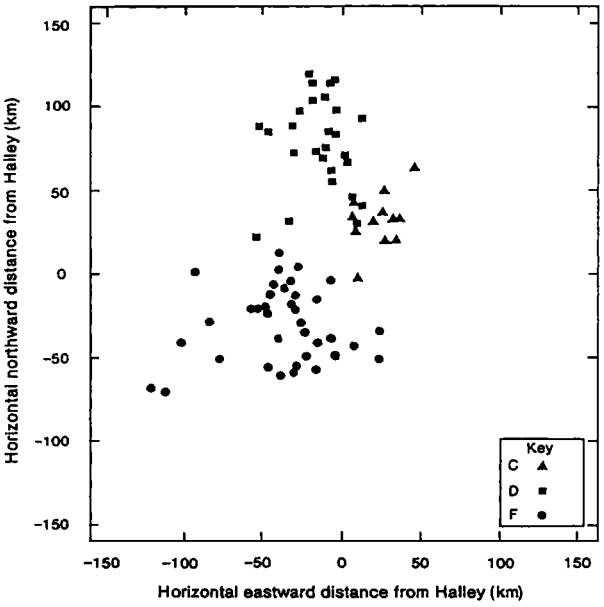

Fig. 3. A 'skymap' representation of the location of the 2.602 MHz echoes received at Halley, Antarctica on 23 June 1982.

the structural shape of the enhancement, the angle from which it is being viewed and the radiowave frequency.

Method 2: Changes In Echo Phase Due To Ionisation Enhancements Along The Echo Path

This method relies on the reception by the ionosonde of a continuous and relatively constant echo from a region of the ionosphere (normally the *F*-region) higher in altitude than the ionisation enhancement. Doolittle [1982] has shown that, in theory, a perturbation in the phase of the totally reflected HF signal will occur if ionisation due to wave-induced precipitation is produced along the reflected ray path. This signature can be detected by measuring the rate-of-change of phase ($\partial\phi/\partial t$) of a reflected echo at a fixed frequency over a suitable interval of time. As a consequence of the density dependence of the refractive index of the ionospheric plasma, changes in the phase of the ordinary mode echo, resulting from changes in the local density along the path, will be in the opposite sense from the density change.

Several instances of a large and sudden decrease in $\partial\phi/\partial t$ were discovered within a 4.2 MHz fixed-frequency sounding which began on 1151:36 UT, at Siple, on 13 November 1982. Six events characterised by a large negative excursion of $\partial\phi/\partial t$ followed by a slow increase to a more positive value than that prevailing prior to the event were found; five of those events occurred during a two minute interval of Siple VLF transmissions specifically designed to induce wave-particle interactions, and hence precipitation. It is notable that for several hours both prior to and after the events, the largest coherent decrease in $\partial\phi/\partial t$ was 90° s^{-1}. By comparison, the

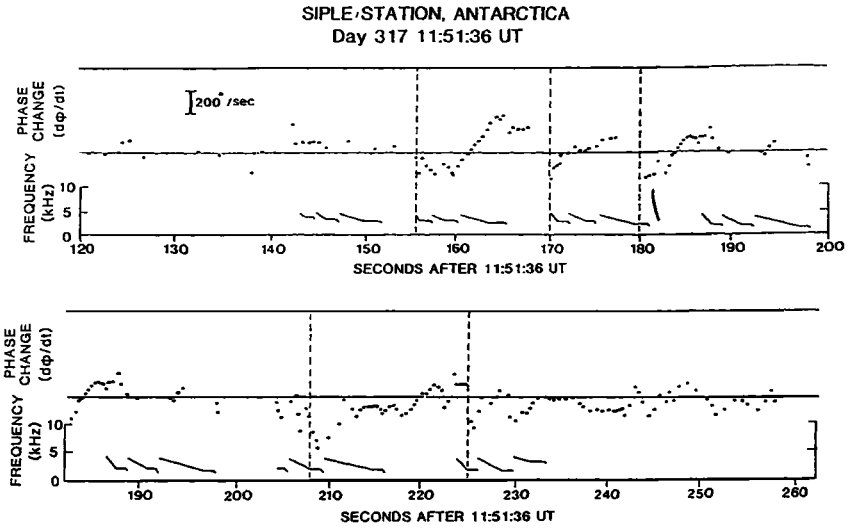

Fig. 4. The rate-of-change of phase of HF transmitter echoes received during a fixed-frequency sounding at 4.2 MHz on 13 November 1982. Below these data are shown the spectra of Siple VLF transmissions and naturally occurring whistler waves. The time is in seconds after 1151:36 UT.

mean decrease in $\partial\phi/\partial t$ for the five events occurring during the VLF transmissions, was 250° s^{-1}. In Figure 4, $\partial\phi/\partial t$ for the 4.2 MHz echoes is displayed together with the frequency format of the Siple VLF transmitter as a function of time from the start of the sounding (1151:36 UT). Each value of $\partial\phi/\partial t$ is a three point running mean (except where breaks in the time series occur); this reduces the influence of occasionally erroneous individual phase measurements which result in one large $\partial\phi/\partial t$ datum followed by an equally large datum of the opposite sign.

In addition to the whistler which occurred on the inter-transmission VLF recording at Siple and which is symbolised at t=182 seconds in Figure 4, whistlers were recorded at Palmer Station, Antarctica (L=2.4), equatorward of Siple, during the Siple transmissions at t=146, 163, 174, 208 and 225 seconds. The VLF spectrograms from Siple also exhibit triggered noise bursts which occur outside the plasmapause and are of the kind which have previously been associated with overhead precipitation at Siple. The simultaneous presence of whistlers, Siple VLF transmissions and triggered emission complicated the process of identifying a definitive source for the precipitation events presented here. Nevertheless, the fact remains that bursts of excess ionisation did occur along the signal ray path during magnetospheric conditions seemingly appropriate to wave-induced precipitation. Five of the six events recorded during a 36 hour interval of essentially continuous operation exceeded the normal variation by a factor of three and occurred during the two minute period when the Siple VLF transmitter was transmitting (in a mode specifically designed to induce such events).

Doolittle [1982] simulated the phase response of a digital ionosonde echo at 1.5 MHz to a five second burst of 1 keV precipitated electrons with an energy flux of 10^{-2} erg cm^{-2} s^{-1} which would produce ionisation near 170 km. This is redrawn in Figure 5a with the ordinate in degrees per second (i.e., $\partial\phi/\partial t$). The phase response can be considered to have three distinct stages. The first, marked 1 on Figure 5a, is the initial rapid decrease in phase. It is dependent on sounding frequency and energy flux, a lower sounding frequency or more energetic flux of electrons resulting in a larger decrease. The second stage response is a function of the duration of the precipitation and the shape of the pulse of electrons. The recovery time (stage 3 in Figure 5) of $\partial\phi/\partial t$ back to a predisturbance level is dependent on the recombination rate and local density. From the rate of recovery, an inference regarding the height of the ionisation enhancement and therefore the energy of the causative precipitation can be made. For the sake of computational efficiency, Doolittle [1982] assumed a square wave pulse of precipitation. Rocket [Rycroft, 1973] and satellite [Voss et al., 1984] measurements show that a precipitation pulse typically consists of a rapid increase (<1.5 s) in flux followed by a relatively slow (≈10 s) decay. Thus the solid line profile of Figure 5a will, in practice, be

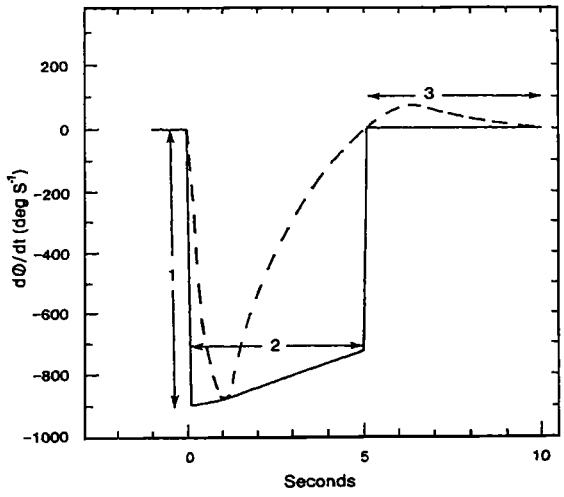

Fig. 5a. Simulated wave-induced precipitation pulse (after Doolittle, 1982) replotted with the ordinate as rate-of-change of phase (solid line). A more realistic precipitation pulse is shown by the dashed line.

asymmetric in time and appear similar to the profile given by the dashed line in Figure 5a. The mean profile derived from the five events occurring between 1154 and 1156 UT is given by the solid line in Figure 5b. The mean decrease (stage 1) in $\partial\phi/\partial t$ was 251±89° s^{-1} with an initial recovery rate of 117±91° s^{-1}. Taking into account the frequency of the measurement, Doolittle's work indicates that an initial decrease in $\partial\phi/\partial t$ of 251° s^{-1} would be produced by a flux of approximately 0.75×10^{-2} erg cm^{-2} s^{-1}. The overlapping data for these events make it difficult to determine the rate of decay of $\partial\phi/\partial t$ (i.e. stage 3). The best estimate is, however, that the time for the enhancement to decay to 1/e of its initial value is ≈26 s (worst estimates between 9 and 145 s). This is similar to that found for Trimpi events and implies particle energies of ≈100 keV [Dingle and Carpenter, 1981].

Discussion

Rycroft [1972] has plotted the variation of the parameter $W_{\|}N$ as a function of L-value, where $W_{\|}$ is the component of the electron energy parallel to the geomagnetic field and N is the number density of the thermal plasma in the wave-particle interaction region. At

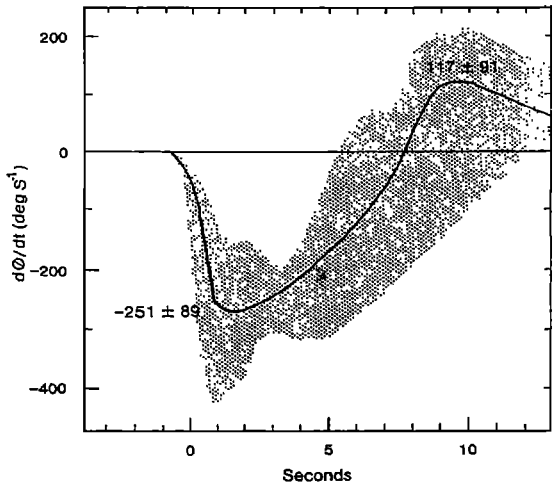

Fig. 5b. The average profile of the change $\partial\phi/\partial t$ derived from the five phase perturbations observed on 13 November 1982 at Siple Station, Antarctica (solid line). The shaded area covers the spread of values from the five events.

L=4.2, $W_{||}N \approx 6000$ keV cm^{-3} for 1 kHz waves and ≈900 keV cm^{-3} for 3 kHz waves. During wave-induced precipitation events, typical electron densities are 10 cm^{-3} poleward and 500 cm^{-3} equatorward of the plasmapause with Siple tending to lie 0.2 to 1.5 L-shells poleward of the plasmapause [Carpenter, 1979]. Thus, the predominant frequency of 3 kHz during the Siple transmission on 13 November 1982 would be in gyroresonance with ≈90 keV electrons outside the plasmapause and ≈2 keV electrons inside the plasmapause. Emissions at 1 kHz would similarly be in resonance with ≈600 keV and ≈12 keV electrons respectively. One potential source of the wave-particle precipitation is the Siple VLF transmitter, which may have induced precipitation either directly, or indirectly via triggered emissions.

Since Halley lies on approximately the same L-shell as Siple, these wave-particle parameters apply there also. The whistler spectrograms show that the whistlers recorded at Halley occurred outside the plasmapause. Whistler F triggered emissions at ≈5.1 kHz (10 s duration) and ≈4.6 kHz (90 s duration). Both of these emission are highly structured, consisting predominantly of hook and riser elements. The extrapolated nose frequency of a potential triggering whistler component, with an upper cutoff near the centre frequency of the longer enduring emission, shows it occurring at L=4.3, almost identical to the L-value indicated by the 'skymap' position of the precipitation occurring during the emission (Figure 3). The parallel energy of ≈40 keV deduced for this precipitation is consistent with production via resonance with whistler waves at 4.6 kHz outside the plasmapause.

The other seven precipitation bursts analysed on the same day have higher particle energies around 80 keV. It may be significant that these all appeared to the north (equatorward) of Halley while the 40 keV event appeared to the south. These more equatorward events would need to be triggered by a lower frequency because of both their high particle energy and the necessarily higher equatorial electron density towards the equator. An emission band is present at ≈2 kHz although there appears to be no direct triggering of that band by the whistlers.

To summarise, initial results from two methods of observing and measuring electron precipitation bursts in the ionosphere using a digital ionosonde have been demonstrated. The evidence suggests that the causal whistler mode waves, while associated with identifiable whistlers or VLF transmissions, are emissions directly triggered by these identifiable sources. Particle energies of 40-100 keV have been deduced. In the first method, the regions over which the precipitation occurs are estimated to be of the order of 30 - 100 km across. Particle fluxes of ≈0.75×10^{-2} erg cm^{-2} s^{-1} were derived from the second method.

Acknowledgements. At Utah State Univ. this research was supported by NSF grants DPP-8308044 and DPP-8418173. NSF grant DPP-8613783 supported the work at Stanford University. The HF sounding radar at Siple Station was operated by S.J. Walter. The facilities at Halley were provided by the British Antarctic Survey.

References

Banks, P.M., C.R. Chappell and A.F. Nagy, A new model for the interaction of auroral electrons with the atmosphere: spectral degradation, backscatter, optical emissions and ionisation, *J. Geophys. Res., 79 (10)*, 1459-1470, 1974.

Belrose, J.S., Radio probing of the ionosphere by the partial reflection of radio waves (from heights below 100 km), *J. Atmos. Terr. Phys., 32*, 567-595, 1970.

Carpenter, D.L., VLF observations of magnetospheric dynamics near the plasmapause, in Magnetospheric Study 1979, *Proc. of the International Workshop on selected Topics of Magnetospheric Physics, Tokyo*, 1979.

Carpenter, D.L., U.S. Inan, M.L. Trimpi, R.A. Helliwell and J.P. Katsufrakis, Perturbations of subionospheric LF and MF signals due to whistler-induced electron precipitation bursts, *J. Geophys. Res., 89 (A11)*, 9857-9862, 1984.

Carpenter, D.L. and J.W. LaBelle, A study of whistlers correlated with bursts of electron precipitation near L=2, *J. Geophys. Res., 87(A6)*, 4427-2234, 1982.

Dingle, B. and D.L. Carpenter, Electron precipitation induced by VLF noise bursts at the plasmapause and detected at conjugate ground stations, *J. Geophys. Res., 86(A6)*, 4597-4606, 1981.

Doolittle, J.H., Modification of the ionosphere by VLF wave-induced electron precipitation, Tech. Report *E4-213012218*, Radio Sci. Lab. Stanford Electron Labs., Stanford Univ., Stanford, CA 94305, 1982.

Grubb, R.N., The NOAA SEL HF Radar (Ionospheric Sounder), NOAA Tech. Memo. *ERL SEL-55*, National Oceanic and Atmos. Admin., Boulder, CO, 1979.

Helliwell, R.A., Low-frequency waves in the magnetosphere, *Reviews of Geophys., 7*, 281-303, 1969.

Helliwell, R.A. and S.B. Mende, Correlation between 4278Å optical emissions and VLF wave events observed at L≈4 in the Antarctic, *J. Geophys. Res., 85*, 3376, 1980.

Inan, U.S., D.L. Carpenter, R.A. Helliwell and J.P. Katsufrakis, Subionospheric VLF/LF phase perturbation produced by lightning-whistler induced particle precipitation, *J. Geophys. Res., 90(A8)*, 7475-7469, 1985.

Jarvis, M.J. and J.R. Dudeney, Reduction of ambiguities in HF radar results through a revised receiving antenna array and sound pattern, *Radio Sci., 21*, 151, 1986.

Rosenberg, T.J., R.A. Helliwell and J.P. Katsufrakis, Electron precipitation associated with discrete VLF emissions, *J. Geophys. Res., 76*, 8445-8452, 1971.

Rycroft, M.J., Enhanced energetic electron intensities at 100 km altitude and a whistler propagating through the plasmasphere, *Planet. Space Sci., 21*, 239-251, 1973.

Rycroft, M.J., VLF emissions in the magnetosphere, *Radio Sci., 7*, 811-830, 1972.

Tsuruda, K., S. Machida, T. Oguti, S. Kokubun, K. Hayashi, T. Kitamura, O. Saka and T. Watanabe, Correlations between the low frequency chorus and pulsating aurora observed by low-light-level television at L≈4.4, *Can. J. Phys., 59*, 1042-1048, 1981.

Voss, H.D., W.L. Imhof, J. Mobilia, E.E. Gaines, M. Walt, U.S. Inan, R.A. Helliwell, D.L. Carpenter, J.P. Katsufrakis, and H.C. Chang, Lightning induced electron precipitation, *Nature, 312*, 740, 1984.

F. T. Berkey, Center for Atmospheric and Space Sciences, Utah State University, Logan, UT 84322-4405.

D. L. Carpenter, STAR Laboratory, Stanford University, Stanford, CA 94305.

M. J. Jarvis and A. J. Smith, British Antarctic Survey, Natural Environment Research Council, High Cross, Madingley Road, Cambridge, CB3 0ET, United Kingdom.

(Received: September 21, 1989;
revised: November 17, 1989:
accepted: November 19, 1989)